Alzheimer's & Dementia: Translational Research & Clinical Interventions 5 (2019) 797-808

Featured Article

Amyloid-β oligomers suppress subunit-specific glutamate receptor increase during LTP

Hiromitsu Tanaka*, Daiki Sakaguchi, Tomoo Hirano

Department of Biophysics, Graduate School of Science, Kyoto University, Sakyo-ku, Kyoto, 606-8502, Japan

Abstract

Introduction: Amyloid-β oligomers (AβOs) are assumed to impair the ability of learning and memory by suppressing the induction of synaptic plasticity, such as long-term potentiation (LTP) in the early stage of Alzheimer's disease. However, the direct molecular mechanism of how AβOs affect excitatory synaptic plasticity remains to be elucidated.

Methods: In order to study the effects of AβOs on LTP-associated changes of AMPA (alpha-amino-3-hydroxy-5-methyl-4-isoxazolepropionic acid)-type glutamate receptor (AMPAR) movement, we performed live-cell imaging of fluorescently labeled AMPAR subunit GluA1 or GluA2 with total internal reflection fluorescence microscopy.

Results: Incubation of cultured hippocampal neurons with AβOs for 1–2 days inhibited the increase in GluA1 number and GluA1 exocytosis frequency in both postsynaptic and extrasynaptic membranes during LTP. In contrast, AβOs did not inhibit the increase in GluA2 number or exocytosis frequency.

Discussion: These results suggest that AβOs primarily inhibit the increase in the number of GluA1 homomers and suppress hippocampal LTP expression.

Keywords: Amyloid-β oligomers; Alzheimer's disease; AMPA-type glutamate receptor; Long-term potentiation; Hippocampus; Exocytosis; Total internal reflection fluorescence microscopy

1. Introduction

Alzheimer's disease (AD) is the most common dementia. The previous study showed that it is too late to treat AD patients after the onset of cell death [1]. Therefore, the therapy should be started at an earlier disease stage when aggregated amyloid-β peptides have still not formed senile plaques [2,3]. Recent studies have suggested that soluble amyloid-β oligomers (AβOs) impair the ability of learning and memory through dysregulation of synaptic plasticity in the hippocampus [4–6]. To obtain a potential clue to find a way to improve the initial deficit of leaning ability, investigating how neurotoxic AβOs alter the synaptic function in early AD has attracted great attention. There are many studies about AβOs-induced intracellular signaling pathways via a variety of synaptic targets of AβOs, such as NMDA (N-methyl-D-aspartate)-type glutamate receptor (NMDAR), metabotropic glutamate receptor 5 and α7 nicotinic acetylcholine receptor, which impair long-term potentiation (LTP) expression [5,7]. Nevertheless, how the location and movement of AMPA (alpha-amino-3-hydroxy-5-methyl-4-isoxazolepropionic acid)-type glutamate receptors (AMPARs) change remains elusive. LTP is a long-lasting enhancement of the postsynaptic response after high-frequency stimulation and has been regarded as a cellular basis of learning and memory [8,9]. For LTP expression, an increase in the surface number of AMPARs is critical. AMPARs are tetramers composed of combinations of four subunits (GluA1-4), and mediate fast

Conflicts of interest: The authors declare no competing financial interests.

*Corresponding author. Tel.: +81 75-753-4238; Fax: +81 75-753-4229.
E-mail address: tanaka@neurosci.biophys.kyoto-u.ac.jp

https://doi.org/10.1016/j.trci.2019.10.003

excitatory synaptic transmission in the central nervous system [10]. In mature hippocampal CA1 neurons, GluA1/GluA2 and GluA2/GluA3 heteromers are predominantly expressed [11,12]. Intriguingly, some studies showed that GluA1 homomers are likely to appear at synapses during the induction of LTP [13–17]. Each type of AMPAR is exocytosed from the inside of dendrites and/or laterally moved from the extrasynaptic membrane to the postsynaptic membrane during LTP [18,19]. It is commonly assumed that there are multiple routes of AMPAR subunit-specific delivery to the postsynaptic membrane during LTP [17,20]. In this study, we focused on hippocampal LTP and attempted to examine the effects of AβOs on LTP-associated AMPARs dynamics. What type of AMPAR movement is suppressed by AβOs? When and where is the movement affected after the LTP-inducing stimulation? There are few reports to precisely evaluate and quantify AMPARs at multiple time points during LTP expression [21].

For addressing these issues, we directly visualized the effects of AβOs on AMPAR movements using total internal reflection fluorescence microscopy (TIRFM). TIRFM makes it possible to detect even a single-molecule signal with a high signal-to-noise ratio by reducing the background fluorescence [22]. In our previous study, we succeeded in the formation of an excitatory postsynaptic-like membrane (PSLM) directly above the glass surface [17,23]. This method has enabled us to accurately measure AMPAR amount in PSLM and to live-cell image the lateral movement and exocytosis of fluorescently labeled AMPARs. Under our experimental conditions, the timing and location of individual exocytosis can be recorded for more than 40 min. Taking advantage of this method, we tried to clarify whether AβOs disturb exocytosis of AMPAR before and after LTP induction in a neural cell culture model of the early stage of AD.

2. Methods

2.1. Animals

All experimental procedures were carried out in accordance with the NIH guide for the care and use of laboratory animals and the ethical guidelines on animal experimentation of Kyoto University and approved by the local committee for handling experimental animals in the Graduate School of Science, Kyoto University.

2.2. Primary cell culture and transfection

The methods for preparing primary cultures of hippocampal neurons and transfection of cDNA were described previously [17,23]. Briefly, hippocampi were dissected out from E18-20 Wistar rat embryos, treated with 0.1% trypsin (Thermo, 15090-046) and dissociated by trituration with a fire-polished Pasteur pipette. Dissociated cells were seeded on poly-D-lysine- (Merck, P7280) and Neurexin (NRX)-coated glass in Neurobasal medium (Thermo, 21103-049) containing 1% penicillin-streptomycin (Thermo, 15140-122), 0.25% glutamine (Merck, G6392) and 2% B27 Electro (Thermo, 17504-044). Detailed procedures for NRX-coating were described in a previous report [23]. Plasmids were transfected into days in vitro 10–15 neurons with Lipofectamine 2000 (Thermo, 11668-019). All imaging experiments were carried out 2–3 days after transfection.

2.3. DNA constructs

Expression vectors for rat GluA1 (flop) or GluA2 (flop) labeled with SEP (super-ecliptic pHluorin) (GluA1-SEP or GluA2-SEP), PSD95 labeled with TagRFPt (PSD95-RFPt), Neuroligin1 with splice insertion A labeled with HA tag (NLG-HA) and NRX1β without splice insertion 4 labeled with human immunoglobulin-Fc region (NRX-Fc) were prepared as described previously [17,23]. Expression vectors for GluA1-or GluA2-SEP (GluA-SEP), PSD95-RFPt, and NLG-HA were transfected into neurons. NRX-Fc vector was transfected into HEK293 cells for purification of NRX-Fc protein. Detailed methods to purify NRX-Fc were reported previously [23]. EGFP expression vector was a generous gift from Professor Y.Tagawa (Kagoshima University, Japan).

2.4. Aβ oligomerization and treatment

AβOs were prepared from lyophilized $A\beta_{1\text{-}42}$ (AnaSpec, AS 20276) using a method similar to those in previous studies [24,25]. Synthetic Aβ peptide was dissolved in 1,1,1,3,3,3-hexafluoro-2-propanol (HFIP) (Wako, 083-04231) to a final concentration of 1 mM and incubated for 2 hr at room temperature (RT, 20–25°C) to yield a solution of monomeric peptide. HFIP was then removed in a rotary evaporator (AS ONE, CVE-1AS), and the dried HFIP film was stored at −80°C. The peptide film was resuspended to make a 5 mM solution in DMSO (Nacalai Tesque, 13445-74), sonicated for 10 min, supplemented with Neurobasal medium to yield a final peptide concentration of 100 μM, sonicated for 20 sec 3 times on ice, and incubated for oligomerization overnight at 4°C. AβOs were added into neuronal cultures to yield a final concentration of 1 μM, which was calculated based on the molecular weight of monomer. Live-cell imaging experiments were performed 1–2 days after the application of AβOs. As controls, reverse $A\beta_{42\text{-}1}$ (AnaSpec, AS-27276) or vehicle was prepared in the same way.

2.5. Western blotting

SDS sample buffer without 2-mercaptoethanol was added to AβOs. Samples were separated by electrophoresis on a 15% polyacrylamide gel and transferred to a PVDF membrane (Merck, IPVH00010). For avoiding nonspecific binding of antibodies, the membrane was blocked with PBS containing 0.1% Tween-20 and 5% skim milk for 30 min at RT. The membrane was immunoblotted using mouse

monoclonal anti-Aβ antibody (BioLegend, 93049, 1:2000) overnight at 4°C, and HRP-conjugated secondary antibody (Jackson ImmunoResearch, 109-035-098, 1:2500) for 1 hr at RT. Bands were detected by using the SuperSignal West Pico Chemiluminescent Substrate (Thermo, 34080).

2.6. Immunocytochemistry

Hippocampal cultured neurons on a poly-D-lysine-coated glass coverslip were fixed in PBS with 4% paraformaldehyde for 10 min. Fixed cells were soaked in PBS with 5% normal goat serum and 0.2% Triton-X for 30 min. Next, they were treated with chick polyclonal anti-GFP antibody (Merck, AB16901, 1:1000) and mouse monoclonal anti-PSD95 (Thermo, MA1-046, 1:500) for 1 hr. Then, samples were labeled with secondary Alexa488-conjugated anti-chick IgG (Thermo, A11039, 1:1000) and Alexa568-conjugated anti-mouse IgG (Thermo, A11031, 1:1000) for 30 min. Fluorescence images were captured using a confocal laser scanning microscope (Olympus, FV1000). Serial confocal images were collected at 0.2 μm intervals to create a Z-axis image stack. All procedures were performed at RT.

2.7. Live-cell imaging and electrical field stimulation

The TIRFM imaging system was composed of an inverted fluorescence microscope (Olympus, IX71) equipped with 100 × NA1.45 TIRFM objective lens, 1.6 × intermediate lens, EM-CCD camera (Andor, iXonEM + DU-897), 488 nm laser (Melles Griot, 85-BCD-020) and 561 nm laser (Coherent, Sapphire 561LP). Data were acquired using MetaMorph software (Molecular Devices). Imaging was performed in the extracellular solution (120 mM NaCl, 2 mM $CaCl_2$, 1 mM $MgCl_2$, 10 mM glucose, 10 mM HEPES-KOH, pH 7.3) at RT.

For calculating the amount of GluA-SEP on the cell surface, fluorescence images were acquired for 100 ms every 20 sec. For detecting individual exocytosis of GluA-SEP, images were acquired for 100 ms every 2 sec, after 30–60 sec of photo-bleaching to improve the signal-to-noise ratio [17,26,27]. In each experiment, an optimized ND filter was used to minimize the effect of photo-bleaching for long-term imaging. Electrical field stimulation (1 ms, 20–26 V/cm, 300 voltage pulses at 50 Hz) was applied to neurons between platinum electrodes.

2.8. Image analysis

Acquired images were analyzed using MetaMorph, ImageJ (NIH), and Excel (Microsoft), as described previously [28]. PSLM area was defined as in a previous study [28]. A dendritic area without the PSD95-RFPt signal was defined as non-PSLM. The frequency of exocytosis was normalized as the number of events/min/25 μm^2. Estimated fluorescence intensity at each time point was normalized by the averaged intensity between 0–3 min before the stimulation (−3–0 min). A spine was defined as a protrusion whose length from a dendrite shaft was no greater than 3 μm. A spine or PSD95 cluster density was calculated as the number per length of a dendrite.

2.9. Statistical analysis

The sample size in each experiment was determined based on previous publications dealing with live-cell imaging [17,26–30]. In each experiment, N indicates the number of cells. All values are presented as mean ± SEM. The equality of SD was assessed by the F test. Statistical tests were performed using Excel and Kyplot (KyensLab).

3. Results

3.1. Effects of Aβ oligomers on spine morphology

AβOs were prepared and characterized by western blotting, as in previous studies [24,25] (Fig. 1A). Bands corresponding to monomer (4.2 kDa), trimer, tetramer, hexamer, and decamer were detected. The most abundant oligomer was tetramer. Next, we applied AβOs to cultured hippocampal neurons expressing EGFP, and immunostained EGFP and endogenous PSD95, a postsynaptic scaffolding protein (Fig. 1B) [31]. One day of incubation with AβOs did not dramatically change the dendritic spine density, whereas 8 days of incubation significantly reduced it (Fig. 1C, Supplementary Table 1). Accordingly, the fluorescent intensity and cluster number of PSD95 were not changed after 1 day of incubation with AβOs, while they were also decreased after 8 days of incubation (Fig. 1C, Supplementary Table 1). These results indicate that AβOs caused dendritic spine retraction, leading to reduction of PSD proteins after 8 days of incubation, but not after 1 day.

3.2. Aβ oligomers suppressed GluA1-SEP increase after LTP induction

We next investigated whether these AβOs inhibit the increase in surface AMPARs during LTP expression. To accurately measure the change of AMPAR amount on the postsynaptic membrane by TIRFM, we formed PSLM on a glass surface coated with Neurexin (NRX) (Fig. 2A). TIRFM selectively visualizes fluorophores localized very close (100 nm) to a glass surface [22]. This area is called the TIRFM visualization zone. NRX is a type of presynaptic adhesion molecule that triggers postsynaptic differentiation through binding to Neuroligin (NLG) [32,33]. PSLM was formed parallel to the glass surface stably as a model of the postsynaptic membrane. Fluorescence signal changes should not have been influenced by the movement of the cell membrane. These conditions enable us to precisely determine AMPAR localization and the signal intensity in PSLM.

We used an expression vector of GluA1 or GluA2, which is a constituent of most of the hippocampal AMPARs [12], labeled with SEP. SEP is a pH-sensitive variant of GFP

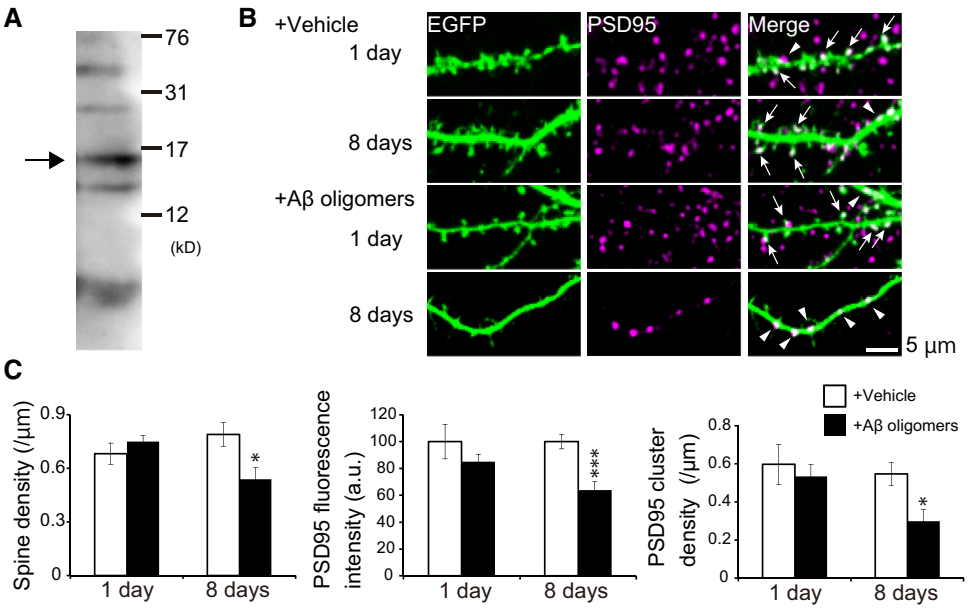

Fig. 1. Excitatory postsynaptic structure degenerated not at 1 day but at 8 days after incubation with AβOs. (A) Western blotting analysis of 1 μM human AβOs. The main oligomer was tetramer (arrow). (B) Representative images of immunostained endogenous PSD95 and EGFP expressed in hippocampal neurons. Application of AβOs for 8 days reduced the number of spines compared with that of the vehicle control. PSD95 clusters were distributed in spines (arrows) and dendritic shafts (arrowheads). (C) Quantification of spine density, fluorescence intensity and cluster number of PSD95 by two-tailed Student's *t* test (N = 7-8 cells, $*P < .05$, $***P < .001$).

that emits little fluorescence when it is in a cytoplasmic vesicle at a low pH, and SEP improves the selective detection of fluorescence on the cell surface at a neutral pH [34]. First, we expressed GluA1-SEP and PSD95-RFPt, and quantified the SEP signal intensity every 20 sec 1–2 days after incubation with AβOs, when most synapses still remain. Then, high-frequency electrical field stimulation to induce LTP was applied to cultured neurons, which causes a rapid increase of the intracellular Ca^{2+} concentration in dendrites [17].

When a preparation was treated with reverse $Aβ_{42-1}$ (revAβ), whose peptide corresponds to the inverted sequence of $Aβ_{1-42}$, GluA1-SEP signal intensity increased at a few minutes after the stimulation in both PSLM and non-PSLM, and the signal intensity remained high (Fig. 2B and C, Supplementary Table 2). The GluA1-SEP signal increase in PSLM tended to be larger than that in non-PSLM, although a significant difference was not detected (Fig. 2B). On the other hand, when cultured neurons were treated with AβOs, the GluA1-SEP signal did not increase after the stimulation but rather decreased for about 10 min and then recovered in both PSLM and non-PSLM (Fig. 2B). Compared with the control condition (revAβ treatment), the GluA1-SEP signal intensity with AβOs was lower in PSLM after the stimulation (Fig. 2C, Supplementary Table 3). Notably, the different effect on GluA1-SEP signal in non-PSLM was detected only at a few minutes after the stimulation (Fig. 2C, Supplementary Table 3). This transient GluA1-SEP decrease after the stimulation may be ascribed to quenching of the intracellular SEP signal in the endoplasmic reticulum (ER) lumen. Previous studies showed that the SEP signal in ER decreases upon intracellular acidification after neuronal activity [28,30]. These results indicate that AβOs inhibited the increase in the number of GluA1-containing receptors in both PSLM and non-PSLM during LTP induction. This effect might be a mechanism of AβOs-mediated impairment of learning-related synaptic plasticity.

3.3. Aβ oligomers did not suppress GluA2-SEP increase after LTP induction

We next investigated whether AβOs inhibited the increase in the amount of GluA2, another type of AMPAR subunit, after LTP induction. In control neurons incubated with revAβ, the GluA2-SEP signal intensity increased gradually after the stimulation in both PSLM and non-PSLM (Fig. 3, Supplementary Table 4). Unexpectedly, even when cultured neurons were incubated with AβOs, the GluA2-SEP signal increased gradually in either area (Fig. 3, Supplementary Table 4). The GluA2-SEP signal increase in AβOs treatment tended to be smaller than that in revAβ treatment, although no significant difference was detected (Fig. 3, Supplementary Table 5). These results indicate that AβOs did not apparently inhibit the increase in the number of GluA2-containing receptors after LTP induction in either PSLM or non-PSLM.

3.4. The increase of GluA1 exocytosis frequency after LTP induction was suppressed by Aβ oligomers

The increase in the amount of GluA1 on the cell surface should be regulated by exocytosis. Taking the results

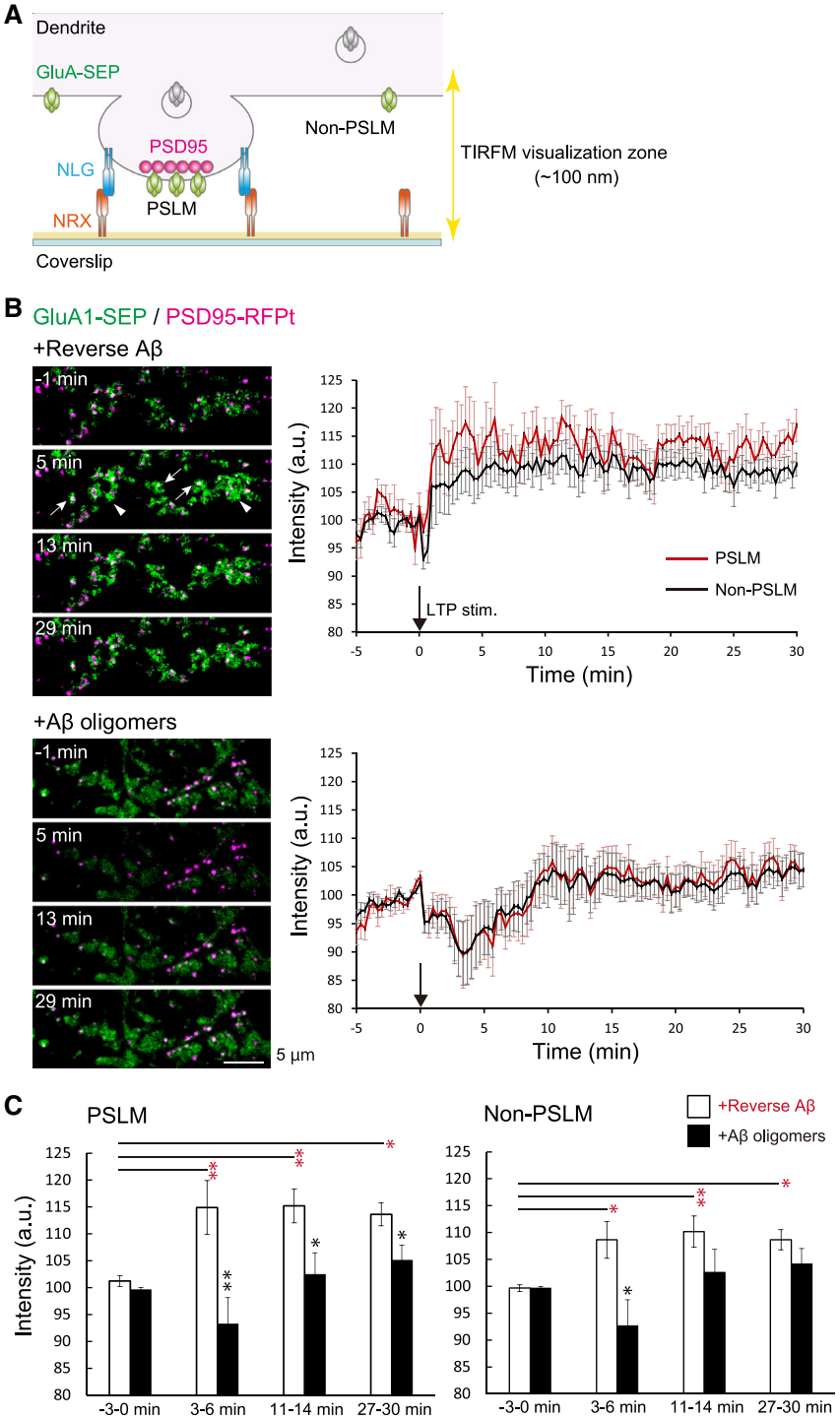

Fig. 2. One to two days of incubation with AβOs impaired LTP-induced increase in the amount of GluA1-SEP in either PSLM or non-PSLM. (A) Schemes of PSLM and live-cell imaging of GluA1 or GluA2 labeled with SEP (GluA-SEP). While GluA-SEP is fluorescent on the cell surface, the fluorescence is quenched in cytoplasmic vesicles at a low pH. TIRF illumination activates fluorescent molecules within the limited Z-axis depth (about 100 nm), enabling high signal-to-noise detection of signals. (B) Representative images (left) of the GluA1-SEP signal (green) and PSD95-RFPt signal (magenta). PSD95-RFPt was recorded before the stimulation and merged with the time-lapse images of GluA1-SEP. In neurons treated with revAβ, the GluA1 signal increased in PSLM (white arrows) and non-PSLM (white arrowheads). Averaged time courses (right) of GluA1-SEP fluorescence intensity in PSLM (red) and non-PSLM (black) measured every 20 sec before and after the LTP stimulation (black arrows). (C) Statistical analyses of data shown in (B). Averaged fluorescence intensity at each time point in 3 min bin. Significant differences between revAβ and AβOs (Benjamin-Hochberg test), or before and after the stimulation (Dunnett's test) are indicated by asterisks (N = 18, 19 cells, $*P < .05$, $**P < .01$).

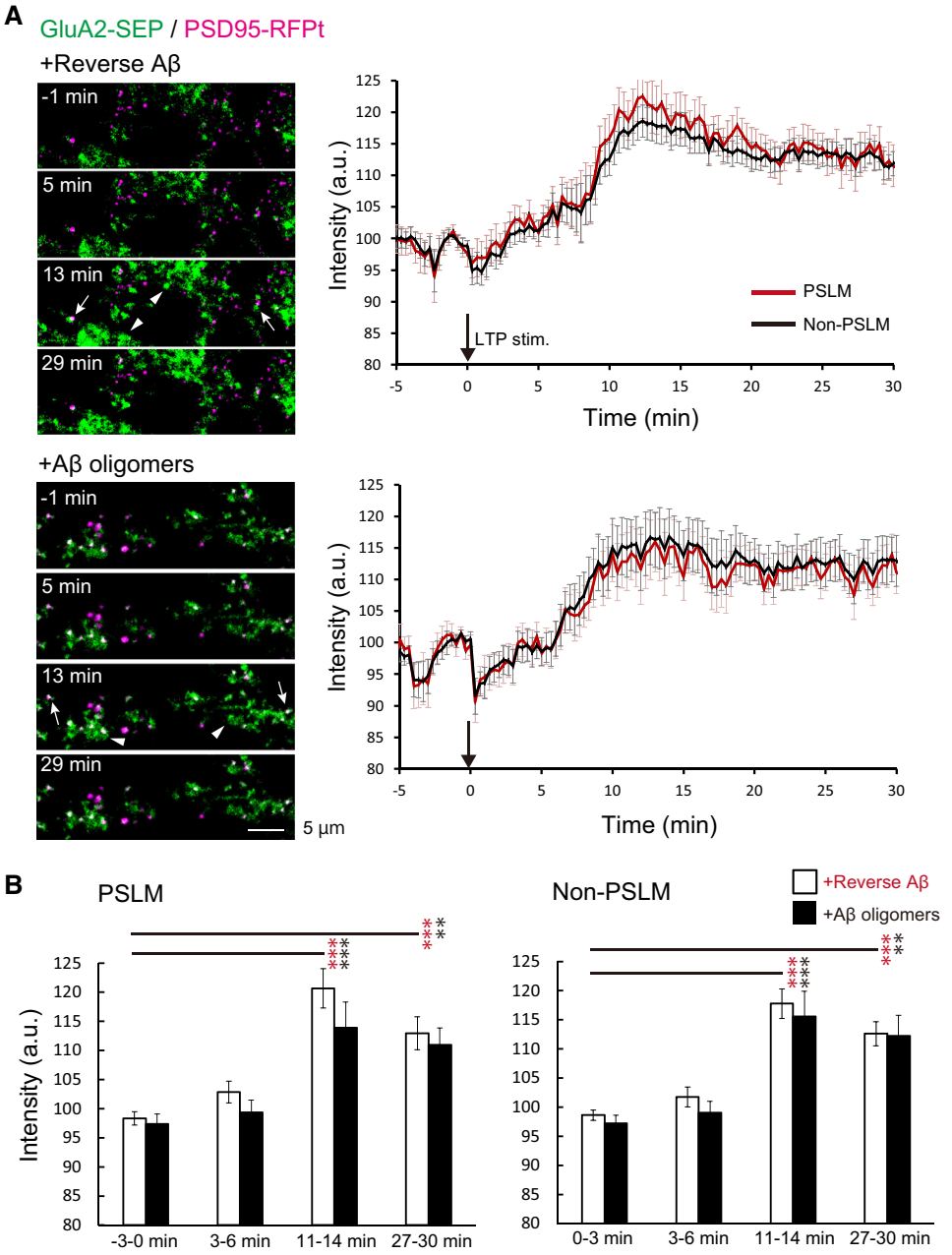

Fig. 3. AβOs did not inhibit the increase in the amount of GluA2-SEP in both PSLM and non-PSLM after LTP-inducing stimulation. (A) Representative images (left) of the GluA2-SEP signal (green) and PSD95-RFPt signal (magenta). PSD95-RFPt was recorded before the stimulation and merged with the time-lapse images of GluA2-SEP. In control neurons treated with revAβ (top), the GluA2 signal increased in PSLM (white arrows) and non-PSLM (white arrowheads). Averaged time courses (right) of GluA2-SEP fluorescence intensity change in PSLM (red) and non-PSLM (black) measured every 20 sec before and after the stimulation (black arrows). (B) Statistical analyses of data in (A). Averaged intensity at each time point in 3 min bin. Significant differences before and after stimulation (Dunnett's test) are indicated by asterisks (N = 17, 19 cells, $^{**}P < .01$, $^{***}P < .001$). No significant difference between revAβ and AβOs (Benjamin-Hochberg test) was detected.

described above into account, we hypothesized that the application of AβOs might affect GluA1 exocytosis during LTP expression. To test this idea, we examined the effects of AβOs on GluA1-SEP exocytosis. We recorded individual exocytosis events in PSLM or non-PSLM and counted the number of events per min before and after the stimulation (Fig. 4A–C). The location of exocytosis was not in the center of PSLM, but in the periphery, as previously reported [17] (Fig. 4A). In control neurons with rev Aβ treatment, the exocytosis frequency transiently increased 0–3 min after the stimulation in both PSLM and non-PSLM compared with that 0–3 min before the stimulation (Fig. 4B and C, Supplementary Table 6). In contrast, the frequency did not change in PSLM or non-PSLM treated with AβOs (Fig. 4B and C, Supplementary Table 6). In PSLM, the exocytosis frequency was significantly lower in

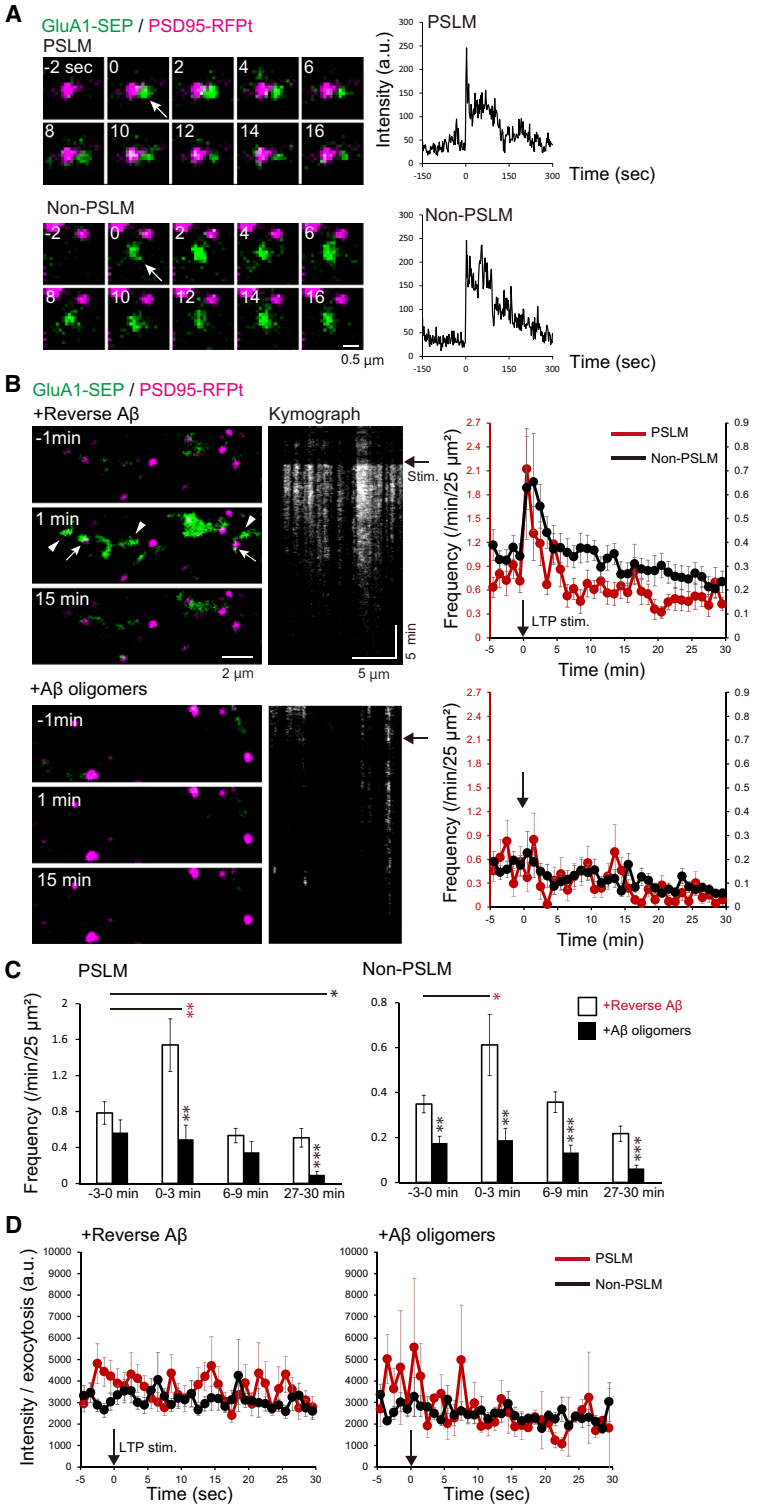

Fig. 4. AβOs abolished LTP-associated GluA1 exocytosis in both PSLM and non-PSLM. (A) Representative GluA1-SEP (green) exocytosis (arrows) in PSLM or non-PSLM (left), and the time courses of GluA1-SEP signal intensity (right) before and after the exocytosis (0 sec). PSD95-RFPt (magenta) was recorded before the stimulation and merged with time-lapse images of GluA1-SEP. The signal increased rapidly and then decreased gradually by lateral diffusion and photo-bleaching. (B) Images of GluA1-SEP and PSD95-RFPt before and after the stimulation (left), and kymographs of GluA1-SEP signals (middle). GluA1 exocytosis occurred in both PSLM (white arrows) and non-PSLM (white arrowheads), particularly 1 min after the stimulation (black arrows). Frequencies of GluA1-SEP exocytosis in PSLN (red, left ordinate) and non-PSLM (black, right ordinate) before and after the stimulation (right). (C) Statistical analyses of data in (B). Significant differences between revAβ and AβOs (Benjamin-Hochberg test), or before and after the stimulation (Dunnett's test) are indicated by asterisks (N = 23, 23 cells, $*P < .05$, $**P < .01$, $***P < .001$). (D) The intensity of the GluA1-SEP signal in each exocytosis in PSLM and non-PSLM before and after the stimulation. No significant difference was detected by Dunnett's test.

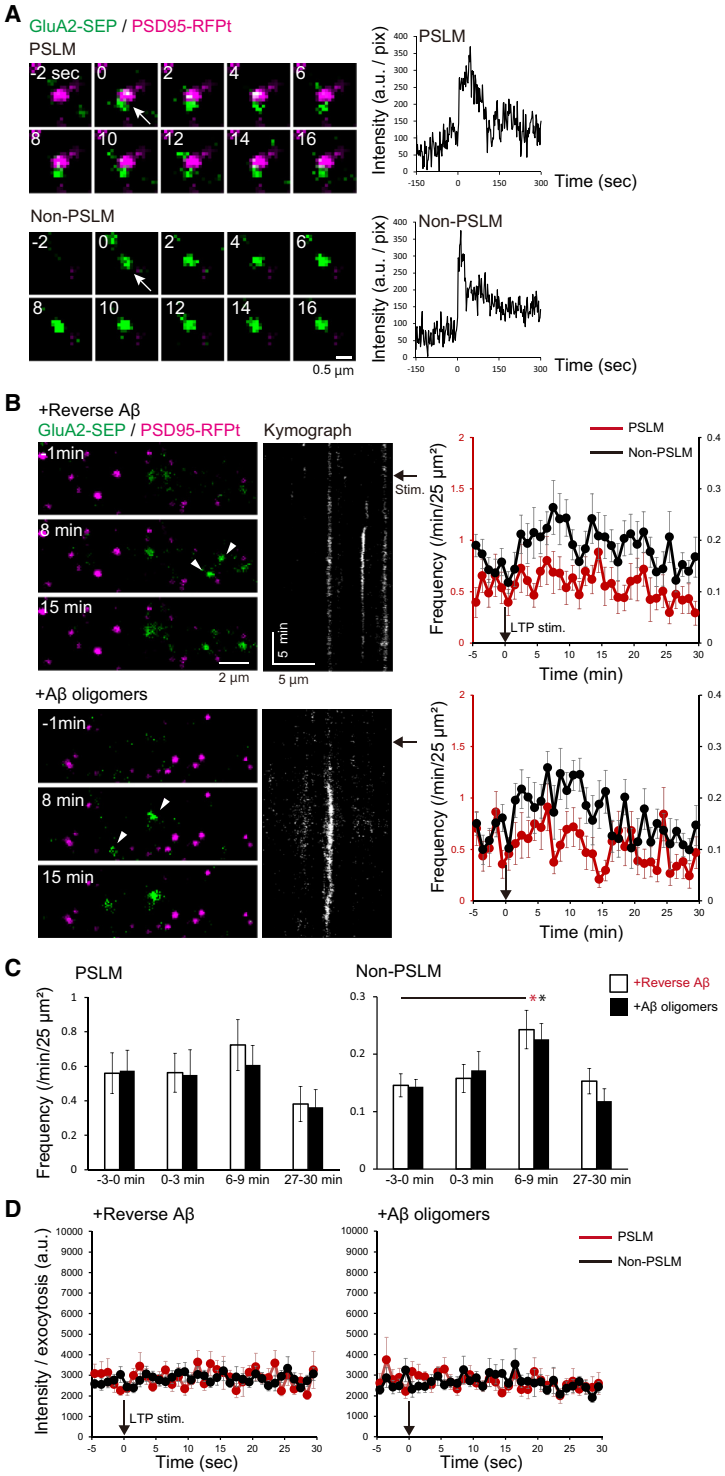

Fig. 5. AβOs did not significantly affect GluA2 exocytosis. (A) Representative GluA2-SEP (green) exocytosis (arrows) in PSLM or non-PSLM (left), and the time courses of GluA2-SEP signal intensity (right) before and after the exocytosis (0 sec). PSD95-RFPt (magenta) was recorded before the stimulation and merged with the time-lapse images of GluA2-SEP. The signal increased rapidly and then decreased gradually by lateral diffusion and photo-bleaching (right). (B) Images of GluA2-SEP and PSD95-RFPt before and after the stimulation (left), and kymographs of GluA2-SEP signals (middle). GluA2 exocytosis occurred in non-PSLM (white arrowheads), especially 8 min after the stimulation (black arrows). Frequencies of GluA2-SEP exocytosis in PSLN (red, left ordinate) and non-PSLM (black, right ordinate) before and after the stimulation (right). (C) Statistical analyses of data in (B). Significant differences before and after stimulation (Dunnett's test) are indicated by asterisks (N = 24, 23 cells, $*P < .05$). No significant difference between revAβ and AβOs (Benjamin-Hochberg test) was detected. (D) The intensity of the GluA2-SEP signal in each exocytosis in PSLM and non-PSLM before and after the stimulation. No significant difference was detected by Dunnett's test.

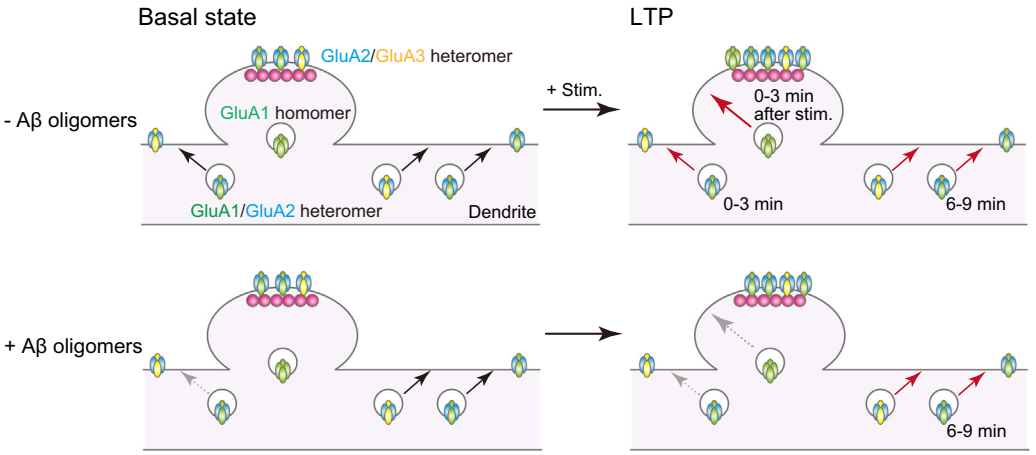

Fig. 6. A hypothetical scheme of dysregulation of AMPAR movement in the early stage of AD. AβOs disturb exocytosis of the GluA1/GluA2 heteromers to the extrasynaptic membrane in a basal condition and in LTP, and suppress exocytosis of GluA1 homomers to the periphery of postsynaptic membrane immediately after LTP-inducing stimulation.

AβOs-treated neurons than that with revAβ 0–3 min and 27–30 min after the stimulation, while the exocytosis frequency with AβOs was significantly lower before and after the stimulation in non-PSLM (Fig, 4C, Supplementary Table 7). Thus, LTP-associated exocytosis of GluA1-containing receptors in PSLM and the basal exocytosis in non-PSLM were suppressed. We did not detect significant differences in the amplitude of exocytosed GluA1-SEP signal before and after the stimulation, in PSLM and non-PSLM, and with AβOs and revAβ treatment (Fig. 4D), suggesting that the number of GluA1 molecules contained in a fusion vesicle is not affected by AβOs and LTP induction. Taking these results together, AβOs selectively suppressed the LTP-associated increase in GluA1 exocytosis frequency.

3.5. The increase of GluA2 exocytosis frequency after LTP induction was not suppressed by Aβ oligomers

We next examined the effects of AβOs on GluA2 exocytosis changes after LTP induction (Fig. 5A–C). In non-PSLM, the exocytosis frequency increased at 6-9 min after the stimulation in neurons treated with either AβOs or revAβ, while there was no significant increase in PSLM at any time points (Fig. 5B and C, Supplementary Table 8). The overall exocytosis frequency in neurons treated with AβOs was similar to that with revAβ (Fig, 5B, Supplementary Table 9). These results indicate that even when neurons were treated with AβOs, the exocytosis of GluA2-containing receptor increased in non-PSLM 6–9 min after the LTP-inducing stimulation. We also noticed that the amount of individual GluA2-SEP released per exocytosis was similar before and after the stimulation, in PSLM and non-PSLM, and with AβOs and revAβ treatment (Fig. 5D). Thus, AβOs did not significantly suppress the increase in GluA2 exocytosis frequency after the LTP-inducing stimulation.

4. Discussion

In this study, we focused on the effects of AβOs on AMPARs to understand the deficits of learning ability at an initial phase of AD. Here, we performed continuous real-time imaging of the effects of AβOs on GluA-SEP with a high spatiotemporal resolution using our original experimental system [17,23]. We showed that AβOs suppressed the increases in GluA1-SEP signal and exocytosis frequency in PSLM, especially right after the LTP-inducing stimulation. AβOs seemed to inhibit the exocytosis of GluA1-containing AMPARs around the postsynaptic membrane in the initial phase of LTP. We also found that AβOs suppressed the basal GluA1-SEP exocytosis in non-PSLM. In contrast, AβOs did not affect GluA2-SEP changes after the stimulation. Thus, the AβOs effect was selective for GluA1 during LTP establishment.

What is different between GluA1 and GluA2? GluA2-containing AMPAR is Ca^{2+} impermeable, while GluA2-lacking AMPAR is Ca^{2+} permeable. The latter also shows higher single-channel conductance [9,19,35]. In the hippocampus, the main GluA2-lacking receptors are likely to be GluA1 homomers, although this idea is still debated [35,36]. Plant et al. (2006) reported a rapid increase of GluA2-lacking AMPARs in the early phase of LTP, followed by replacement by GluA2-containing AMPARs [13]. Previous studies showed direct incorporation of GluA1 into postsynaptic structures during LTP [14–17,29,37,38]. In particular, using the same preparation as that used here, we demonstrated that GluA1 homomers were directly exocytosed to PSLM, while GluA1/GluA2 heteromers were exocytosed to non-PSLM, immediately after the LTP-inducing stimulation [17]. Here, we showed that AβOs suppressed the GluA1-SEP increase but not the GluA2-SEP increase after the LTP-inducing stimulation. Taking all these findings together, we would like to propose the following hypothetical model for postsynaptic dysfunction in the early stage of

AD (Fig. 6). AβOs inhibit the exocytosis of GluA1 homomers into the vicinity of postsynaptic membrane in the initial phase of LTP, impairing LTP induction. AβOs do not disturb the increase in GluA2-containing AMPARs, such as GluA1/GluA2 and/or GluA2/GluA3 heteromers around 6–9 min after LTP induction. We also showed that AβOs inhibit both basal and LTP-associated GluA1-SEP exocytosis in the extrasynaptic membrane, which would supply the extrasynaptic pool of surface GluA1/GluA2 heteromers. The slightly lower increase of GluA2-SEP in neurons treated with AβOs than in those with revAβ might reflect suppression of exocytosis of GluA1/GluA2 heteromers (Fig. 3).

Why do AβOs preferentially block the increase of GluA1, but not GluA2? AMPAR subunits are divergent in amino-acid sequences of extracellular amino-terminal domains (ATDs) and cytoplasmic carboxy-terminal domains (CTDs) [19,39]. LTP induction in a CA1 pyramidal neuron depends on NMDAR causing Ca^{2+} influx, which subsequently activates protein kinases, such as CaMKII and PKC [40,41]. It is well known that CaMKII and PKC directly phosphorylate GluA1 S818 and S831 at CTDs, which increases GluA1 single-channel conductance and promotes GluA1 targeting to PSD. It is possible that extracellular AβOs interact with NMDAR and cause Ca^{2+} dysregulation [7,42,43]. This might cause aberrant activation of CaMKII, PKC, or calcineurin, which leads to AMPAR destabilization or internalization, precluding GluA1 exocytosis from contributing to LTP establishment [21,44]. On the other hand, recent studies showed that the ATDs of GluA1, but not GluA2, are necessary for targeting and retention of AMPARs at synapses during LTP [45,46]. Extracellular AβOs might bind to ATDs of GluA1 and prevent the incorporation of GluA1-containing receptors into the plasma membrane by an unknown mechanism. Alternatively, extracellular AβOs might be taken up into neurons, and the internalized AβOs might directly or indirectly disturb the interaction between the CTDs of GluA1 and kinases, inhibiting GluA1 exocytosis [47]. We also note that Whitcomb et al. (2015) reported that intracellular infusion of oligomerized Aβ caused the insertion of GluA1, but not GluA2, into the postsynaptic membrane through PKA-dependent phosphorylation [48]. This increase in the number of GluA1 on the postsynaptic membrane caused by AβOs might occlude GluA1 exocytosis during LTP.

Certainly, PSLM is an artificial structure and might not express all normal postsynaptic functions. However, postsynaptic proteins, such as PSD95 and homer, accumulate in PSLM, and dynamic changes of AMPARs occur there during LTP, as reported previously [17,23]. In addition, normal synapses in a conventional culture preparation show qualitatively similar dynamic changes of GluA1 to those observed in PSLM during long-term depression [28]. Taking all these facts together, we suggest that PSLM retains critical properties related to synaptic plasticity. We have recently developed methods to visualize individual endocytosis events, and also to form active-zone like membrane on an NLG-coated glass surface [49,50]. These methods could also be useful for analyzing the effects of AβOs on endocytosis of AMPARs and presynaptic function in future studies.

Acknowledgments

We thank Dr. S. Kawaguchi for critical comments on the manuscript and Dr. E. Nakajima for proofreading the manuscript. This work was supported by grants 25110717 to T.H. and 17H05697 to H.T. from the Ministry of Education, Culture, Sports, Science and Technology in Japan, grants 15H04259 and 18H02526 to T.H. and 18K14817 to H.T. from the Japan Society for the Promotion of Science, and grants to H.T. from the Naito Foundation, Takeda Science Foundation, and Kyoto University Foundation in Japan.

Supplementary data

Supplementary data related to this article can be found at https://doi.org/10.1016/j.trci.2019.10.003.

RESEARCH IN CONTEXT

1. Systematic review: Amyloid-β oligomers (AβOs) impair the ability of learning and memory by suppressing induction of synaptic plasticity, such as hippocampal long-term potentiation (LTP) in the early stage of Alzheimer's disease (AD). However, little is known about the pathological effects of AβOs on LTP-associated changes of AMPA-type glutamate receptor (AMPAR) amount and exocytosis at the stage before the occurrence of spine retraction.
2. Interpretation: We visualized the location and movement of AMPAR subunit GluA1 or GluA2 with a high spatiotemporal resolution, and showed that AβOs preferentially suppress the LTP-associated increase in surface amount and exocytosis of GluA1 (but not GluA2) into postsynaptic and extrasynaptic membranes.
3. Future directions: Our findings raise the possibility that AβOs preferentially inhibit the increase in exocytosis of GluA1 homomers into the postsynaptic membrane and suppress the hippocampal LTP expression. Clarification of how AβOs specifically affect GluA1 exocytosis might contribute to therapy for mild memory impairment in early AD.

References

[1] Holmes C, Boche D, Wilkinson D, Yadegarfar G, Hopkins V, Bayer A, et al. Long-term effects of Abeta42 immunisation in Alzheimer's disease: follow-up of a randomised, placebo-controlled phase I trial. Lancet 2008;372:216–23.

[2] Holtzman DM, Morris JC, Goate AM. Alzheimer's disease: the challenge of the second century. Sci Transl Med 2011;3:77sr1.

[3] Suzuki K, Iwata A, Iwatsubo T. The past, present, and future of disease-modifying therapies for Alzheimer's disease. Proc Jpn Acad Ser B Phys Biol Sci 2017;93:757–71.

[4] Mucke L, Selkoe DJ. Neurotoxicity of amyloid beta-protein: synaptic and network dysfunction. Cold Spring Harb Perspect Med 2012; 2:a006338.

[5] Benilova I, Karran E, De Strooper B. The toxic Abeta oligomer and Alzheimer's disease: an emperor in need of clothes. Nat Neurosci 2012;15:349–57.

[6] Takashima A. Amyloid-beta, tau, and dementia. J Alzheimer's Dis 2009;17:729–36.

[7] Jarosz-Griffiths HH, Noble E, Rushworth JV, Hooper NM. Amyloid-beta receptors: The good, the bad, and the prion protein. J Biol Chem 2016;291:3174–83.

[8] Bliss TV, Collingridge GL. A synaptic model of memory: long-term potentiation in the hippocampus. Nature 1993;361:31–9.

[9] Malinow R, Malenka RC. AMPA receptor trafficking and synaptic plasticity. Annu Rev Neurosci 2002;25:103–26.

[10] Dingledine R, Borges K, Bowie D, Traynelis SF. The glutamate receptor ion channels. Pharmacol Rev 1999;51:7–61.

[11] Wenthold RJ, Petralia RS, Blahos J II, Niedzielski AS. Evidence for multiple AMPA receptor complexes in hippocampal CA1/CA2 neurons. J Neurosci 1996;16:1982–9.

[12] Lu W, Shi Y, Jackson AC, Bjorgan K, During MJ, Sprengel R, et al. Subunit composition of synaptic AMPA receptors revealed by a single-cell genetic approach. Neuron 2009;62:254–68.

[13] Plant K, Pelkey KA, Bortolotto ZA, Morita D, Terashima A, McBain CJ, et al. Transient incorporation of native GluR2-lacking AMPA receptors during hippocampal long-term potentiation. Nat Neurosci 2006;9:602–4.

[14] Clem RL, Huganir RL. Calcium-permeable AMPA receptor dynamics mediate fear memory erasure. Science 2010;330:1108–12.

[15] Guire ES, Oh MC, Soderling TR, Derkach VA. Recruitment of calcium-permeable AMPA receptors during synaptic potentiation is regulated by CaM-kinase I. J Neurosci 2008;28:6000–9.

[16] Yang Y, Wang XB, Zhou Q. Perisynaptic GluR2-lacking AMPA receptors control the reversibility of synaptic and spines modifications. Proc Natl Acad Sci U S A 2010;107:11999–2004.

[17] Tanaka H, Hirano T. Visualization of subunit-specific delivery of glutamate receptors to postsynaptic membrane during hippocampal long-term potentiation. Cell Rep 2012;1:291–8.

[18] Kennedy MJ, Ehlers MD. Mechanisms and function of dendritic exocytosis. Neuron 2011;69:856–75.

[19] Diering GH, Huganir RL. The AMPA receptor code of synaptic plasticity. Neuron 2018;100:314–29.

[20] Shi S, Hayashi Y, Esteban JA, Malinow R. Subunit-specific rules governing AMPA receptor trafficking to synapses in hippocampal pyramidal neurons. Cell 2001;105:331–43.

[21] Opazo P, Viana da Silva S, Carta M, Breillat C, Coultrap SJ, Grillo-Bosch D, et al. CaMKII metaplasticity drives Abeta oligomer-mediated synaptotoxicity. Cell Rep 2018;23:3137–45.

[22] Axelrod D. Total internal reflection fluorescence microscopy in cell biology. Traffic 2001;2:764–74.

[23] Tanaka H, Fujii S, Hirano T. Live-cell imaging of receptors around postsynaptic membranes. Nat Protoc 2014;9:76–89.

[24] Ferreira IL, Bajouco LM, Mota SI, Auberson YP, Oliveira CR, Rego AC. Amyloid beta peptide 1-42 disturbs intracellular calcium homeostasis through activation of GluN2B-containing N-methyl-d-aspartate receptors in cortical cultures. Cell Calcium 2012;51:95–106.

[25] Ryan DA, Narrow WC, Federoff HJ, Bowers WJ. An improved method for generating consistent soluble amyloid-beta oligomer preparations for in vitro neurotoxicity studies. J Neurosci Methods 2010; 190:171–9.

[26] Araki Y, Lin DT, Huganir RL. Plasma membrane insertion of the AMPA receptor GluA2 subunit is regulated by NSF binding and Q/R editing of the ion pore. Proc Natl Acad Sci U S A 2010; 107:11080–5.

[27] Lin DT, Makino Y, Sharma K, Hayashi T, Neve R, Takamiya K, et al. Regulation of AMPA receptor extrasynaptic insertion by 4.1N, phosphorylation and palmitoylation. Nat Neurosci 2009;12:879–87.

[28] Fujii S, Tanaka H, Hirano T. Suppression of AMPA receptor exocytosis contributes to hippocampal LTD. J Neurosci 2018;38:5523–37.

[29] Kennedy MJ, Davison IG, Robinson CG, Ehlers MD. Syntaxin-4 defines a domain for activity-dependent exocytosis in dendritic spines. Cell 2010;141:524–35.

[30] Rathje M, Fang H, Bachman JL, Anggono V, Gether U, Huganir RL, et al. AMPA receptor pHluorin-GluA2 reports NMDA receptor-induced intracellular acidification in hippocampal neurons. Proc Natl Acad Sci U S A 2013;110:14426–31.

[31] Okabe S. Molecular anatomy of the postsynaptic density. Mol Cell Neurosci 2007;34:503–18.

[32] Graf ER, Zhang X, Jin SX, Linhoff MW, Craig AM. Neurexins induce differentiation of GABA and glutamate postsynaptic specializations via neuroligins. Cell 2004;119:1013–26.

[33] Südhof TC. Neuroligins and neurexins link synaptic function to cognitive disease. Nature 2008;455:903–11.

[34] Miesenböck G, De Angelis DA, Rothman JE. Visualizing secretion and synaptic transmission with pH-sensitive green fluorescent proteins. Nature 1998;394:192–5.

[35] Adesnik H, Nicoll RA. Conservation of glutamate receptor 2-containing AMPA receptors during long-term potentiation. J Neurosci 2007;27:4598–602.

[36] Gray EE, Fink AE, Sarinana J, Vissel B, O'Dell TJ. Long-term potentiation in the hippocampal CA1 region does not require insertion and activation of GluR2-lacking AMPA receptors. J Neurophysiol 2007; 98:2488–92.

[37] Kopec CD, Li B, Wei W, Boehm J, Malinow R. Glutamate receptor exocytosis and spine enlargement during chemically induced long-term potentiation. J Neurosci 2006;26:2000–9.

[38] Wu D, Bacaj T, Morishita W, Goswami D, Arendt KL, Xu W, et al. Postsynaptic synaptotagmins mediate AMPA receptor exocytosis during LTP. Nature 2017;544:316–21.

[39] Zhou Z, Liu A, Xia S, Leung C, Qi J, Meng Y, et al. The C-terminal tails of endogenous GluA1 and GluA2 differentially contribute to hippocampal synaptic plasticity and learning. Nat Neurosci 2018; 21:50–62.

[40] Kristensen AS, Jenkins MA, Banke TG, Schousboe A, Makino Y, Johnson RC, et al. Mechanism of Ca2+/calmodulin-dependent kinase II regulation of AMPA receptor gating. Nat Neurosci 2011;14:727–35.

[41] Derkach VA, Oh MC, Guire ES, Soderling TR. Regulatory mechanisms of AMPA receptors in synaptic plasticity. Nat Rev Neurosci 2007;8:101–13.

[42] Kodis EJ, Choi S, Swanson E, Ferreira G, Bloom GS. N-methyl-D-aspartate receptor-mediated calcium influx connects amyloid-beta oligomers to ectopic neuronal cell cycle reentry in Alzheimer's disease. Alzheimers Dement 2018;14:1302–12.

[43] Sinnen BL, Bowen AB, Gibson ES, Kennedy MJ. Local and use-dependent effects of beta-amyloid oligomers on NMDA receptor function revealed by optical quantal analysis. J Neurosci 2016; 36:11532–43.

[44] Zhao WQ, Santini F, Breese R, Ross D, Zhang XD, Stone DJ, et al. Inhibition of calcineurin-mediated endocytosis and alpha-amino-3-hydroxy-5-methyl-4-isoxazolepropionic acid (AMPA) receptors

prevents amyloid beta oligomer-induced synaptic disruption. J Biol Chem 2010;285:7619–32.

[45] Watson JF, Ho H, Greger IH. Synaptic transmission and plasticity require AMPA receptor anchoring via its N-terminal domain. Elife 2017;6.

[46] Diaz-Alonso J, Sun YJ, Granger AJ, Levy JM, Blankenship SM, Nicoll RA. Subunit-specific role for the amino-terminal domain of AMPA receptors in synaptic targeting. Proc Natl Acad Sci U S A 2017;114:7136–41.

[47] LaFerla FM, Green KN, Oddo S. Intracellular amyloid-beta in Alzheimer's disease. Nat Rev Neurosci 2007;8:499–509.

[48] Whitcomb DJ, Hogg EL, Regan P, Piers T, Narayan P, Whitehead G, et al. Intracellular oligomeric amyloid-beta rapidly regulates GluA1 subunit of AMPA receptor in the hippocampus. Sci Rep 2015;5:10934.

[49] Fujii S, Tanaka H, Hirano T. Detection and characterization of individual endocytosis of AMPA-type glutamate receptor around postsynaptic membrane. Genes Cells 2017;22:583–90.

[50] Funahashi J, Tanaka H, Hirano T. Visualization of synchronous or asynchronous release of single synaptic vesicle in active-zone-like membrane formed on neuroligin-coated glass surface. Front Cell Neurosci 2018;12:140.